Engineering

Electrical Engineering fields

Okayama University *Year* 1997

An approach to harmonic current-free AC/DC power conversion for large industrial loads: the integration of a series active filter with a double-series diode rectifier

Hideaki Fujita
Okayama University

Hirofumi Akagi
Okayama University

http://escholarship.lib.okayama-u.ac.jp/electrical_engineering/13

An Approach to Harmonic Current-Free AC/DC Power Conversion for Large Industrial Loads: The Integration of a Series Active Filter with a Double-Series Diode Rectifier

Hideaki Fujita, *Member, IEEE,* and Hirofumi Akagi, *Fellow, IEEE*

***Abstract*— This paper proposes a new harmonic current-free ac/dc power conversion system characterized by the integration of a small-rated series active filter with a large-rated double-series diode rectifier. The dc terminals of the active filter are directly connected in parallel with those of the diode rectifier, thereby forming a common dc bus. The active filter enables the diode rectifier to draw three-phase sinusoidal currents from the utility. In addition, it can provide the supplementary value-added function of regulating the common dc-bus voltage to a limited extent of ±5%, slightly increasing the rms voltage rating, but not increasing the peak voltage rating. Experimental results obtained from a 5-kW laboratory system verify the practical viability and cost effectiveness of the proposed system.**

***Index Terms*— Diode rectifiers, harmonic currents, PWM inverters, series active filters.**

I. INTRODUCTION

VOLTAGE harmonics in power transmission/distribution systems have become a serious problem in many countries, with the proliferation of power electronics equipment into industry. Generally, individual electric power consumers are responsible for limiting current harmonics because voltage harmonics result from the current harmonics produced by their own power electronics equipment. The guidelines for harmonic mitigation, enacted on Oct. 3, 1994 in Japan, are currently applied on a voluntary basis to keep current harmonics in check.

Harmonic current-free rectifiers capable of operating at unity power factor are required as utility interfaces for inverter-based industrial loads such as adjustable-speed motor drives and uninterruptible power supplies in a range of 1–10 MW. Recently, pulsewidth modulation (PWM) rectifiers consisting of the same power circuit topology as PWM inverters have shown promise of meeting the guidelines for harmonic mitigation [1]–[4]. The increased cost and loss caused by PWM, however, would make a high-power PWM rectifier rated at 1–10 MW economically impractical. The reason is that GTO thyristors or IGBT's used for the PWM rectifier are subjected to high-frequency switching of the full amount of active power which is delivered to an inverter-based load connected on the dc side of the rectifier, even if no reactive power is handled by the switching devices.

This paper proposes a new ac/dc power conversion system providing a solution to the above-mentioned problems hidden in the PWM rectifier. A small-rated series active filter [5] for the purpose of achieving both harmonic compensation and dc voltage regulation is integrated with a large-rated double-series diode rectifier for the purpose of performing ac/dc power conversion. The dc terminals of the active filter are directly connected in parallel with those of the diode rectifier, thereby forming a common dc bus [6]. The active filter shares an electrolytic dc capacitor with the diode rectifier, so that no dc capacitor is required for the active filter, except for a small high-frequency capacitor.

The active filter with an rms voltage rated at 5% and with a peak voltage rated at 7.6% enables the diode rectifier to draw three-phase sinusoidal currents from the utility. In addition, it can provide the supplementary value-added function of regulating the common dc-bus voltage to a limited extent of ±5%, slightly increasing the rms voltage rating but not increasing the peak voltage rating. The function of achieving not only harmonic compensation, but also dc-bus voltage regulation, justifies the integration of the active filter with the diode rectifier practically and economically.

II. SYSTEM CONFIGURATION

Fig. 1 shows a new harmonic current-free ac/dc power conversion system proposed and developed in this paper. It consists of the combination of a double-series diode rectifier of 5 kW and a series active filter with a peak voltage and current rating of 0.38 kVA. The ac terminals of a single-phase H-bridge voltage-fed PWM inverter are connected in "series" with a power line through a single-phase matching transformer, so that the combination of the matching transformers and the PWM inverters forms the "series" active filter. For small- to medium-power systems, it is economically practical to replace the three single-phase inverters with a single three-phase inverter using six insulated gate bipolar transistors (IGBT's). A small-rated high-pass filter for suppression of switching ripples

---

Paper IPCSD 97–30, presented at the 1996 Industry Applications Society Annual Meeting, San Diego, CA, October 6–10, and approved for publication in the IEEE TRANSACTIONS ON INDUSTRY APPLICATIONS by the Industrial Power Converter Committee of the Industry Applications Society. Manuscript released for publication May 7, 1997.

The authors are with the Department of Electrical Engineering, Okayama University, Okayama-City 700, Japan.

Publisher Item Identifier S 0093-9994(97)06565-1.

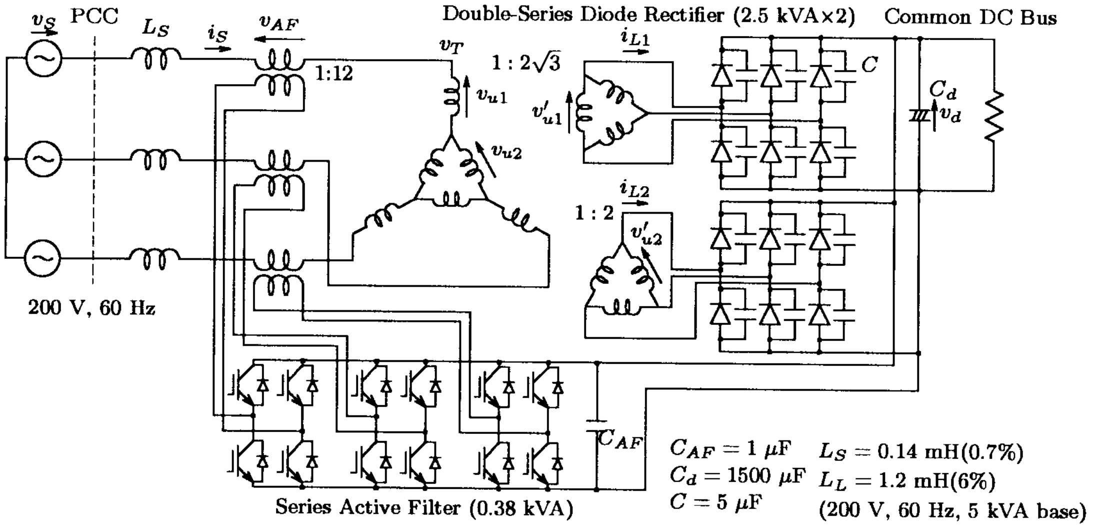

Fig. 1. Experimental system of the proposed ac/dc power conversion system.

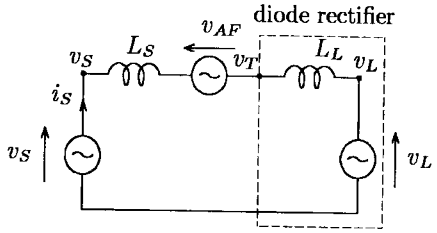

Fig. 2. Single-phase equivalent circuit for the proposed system.

[7] is connected to the ac terminals of each inverter in the experimental system, although it is eliminated from Fig. 1 for the sake of simplicity.

The primary windings of the Y–Δ and Δ–Δ connected transformers are connected in "series" with each other, so that the combination of the three-phase transformers and two three-phase diode rectifiers forms the "double-series" diode rectifier which is characterized as a three-phase twelve-pulse rectifier. The dc terminals of the diode rectifier and the active filter form a common dc bus equipped with an electrolytic capacitor. This results not only in eliminating any electrolytic capacitor from the active filter, but also in reducing current ripples flowing into the electrolytic capacitor across the common dc bus.

Connecting only a commutation capacitor C in parallel with each diode plays an essential role in reducing the required peak voltage rating of the series active filter, as discussed later.

III. OPERATING PRINCIPLE

Fig. 2 shows an equivalent circuit for the proposed system on a per-phase basis. The series active filter [5]–[10] is represented as an ac voltage source v_{AF} and the double-series diode rectifier as the series connection of a leakage inductor L_L of the transformers with an ac voltage source v_L. The reason for providing the ac voltage source to the equivalent model of the diode rectifier is that the electrolytic capacitor C_d is directly connected to the dc terminals of the diode rectifier, as shown in Fig. 1.

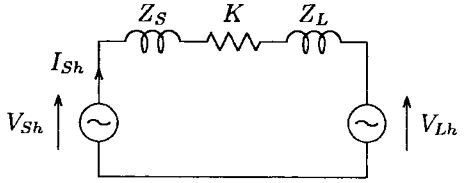

Fig. 3. Single-phase equivalent circuit with respect to harmonics.

The active filter is controlled in such a way as to present zero impedance for the fundamental frequency and to act as a resistor with high resistance of $K\,[\Omega]$ for harmonic frequencies. The ac voltage of the active filter, which is applied to a power line through the matching transformer, is given by

$$v_{\mathrm{AF}}^{*} = K \cdot i_{Sh} \tag{1}$$

where i_{Sh} is a supply harmonic current drawn from the utility. Note that v_{AF} and i_{Sh} are instantaneous values. Fig. 3 shows an equivalent circuit with respect to current and voltage harmonics in Fig. 2. Reference to Fig. 3 enables derivation of the following basic equations:

$$I_{Sh} = \frac{V_{Sh} - V_{Lh}}{Z_S + Z_L + K} \tag{2}$$

$$V_{\mathrm{AF}} = \frac{K}{Z_S + Z_L + K}\,(V_{Sh} - V_{Lh}) \tag{3}$$

where V_{AF} is equal to the harmonic voltage appearing across the resistor K in Fig. 3.

If $K \gg Z_S + Z_L$, (2) and (3) are changed into the following simple equations:

$$I_{Sh} \approx 0 \tag{4}$$

$$V_{\mathrm{AF}} \approx V_{Sh} - V_{Lh}. \tag{5}$$

Equation (4) implies that an almost purely sinusoidal current is drawn from the utility. As a result, each diode in the diode rectifier continues conducting during a half cycle. Equation (5) suggests that the harmonic voltage V_{Lh}, which is produced by the diode rectifier, appears at the primary terminals of the

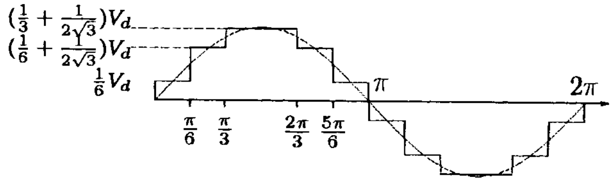

Fig. 4. Synthesized ac voltage v_L of the double-series three-phase twelve-pulse diode rectifier without commutation capacitor.

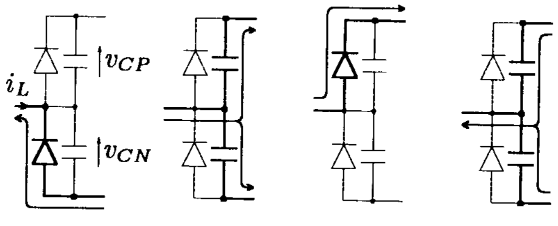

(a) (b) (c) (d)

Fig. 5. Operating principle of the commutation capacitors.

transformers in Fig. 1, although it does not appear upstream of the active filter or at the utility-consumer point of common coupling (PCC).

Fig. 4 shows a synthesized ac voltage of the diode rectifier without commutation capacitors, assuming the active filter to be operating. The waveform of the synthesized ac voltage v_L would be equal to the voltage waveform of the primary terminals, v_T, of the transformers, if the leakage inductance L_L of the transformers were neglected. Each harmonic voltage in v_L is given as follows:

$$v_L = \frac{2V_d}{\pi}\left(\sin \omega t + \frac{1}{11}\sin 11\omega t + \frac{1}{13}\sin 13\omega t + \cdots\right). \tag{6}$$

The eleventh and thirteenth harmonic to fundamental voltage ratios in v_L are 9 and 7.7%, respectively. The total harmonic distortion of the supply voltage upstream of the PCC would be less than 3% in typical industrial power systems. This suggests that v_{Lh} is more dominant in determining the peak voltage rating of the series active filter than is v_{Sh}. Fig. 4 suggests that a step change in the synthesized ac voltage occurs at every instant of commutation, thus requiring the active filter to provide a high peak voltage rating.

IV. EFFECT OF COMMUTATION CAPACITORS

Fig. 5 shows the operating principle of commutation on a per-phase basis, where a commutation capacitor is connected across each diode of the rectifier with a dc capacitor, but without a dc inductor. Fig. 6 shows the waveforms of the ac current i_L, the commutation capacitor voltages v_{CP} and v_{CN}, and the synthesized ac voltage v_L. Let us consider commutation from the lower diode to the upper diode, assuming i_L to be a sinusoidal current. Before the commutation, i_L flows through the lower diode with the capacitor voltages of $v_{CP} = V_d$ and $v_{CN} = 0$, as shown in Figs. 5(a) and 6(a).

When the polarity of i_L changes from the negative to the positive, i_L begins to flow through the upper and lower commutation capacitors, which act like bypass capacitors, as shown in Figs. 5(b) and 6(b). As long as half of i_L discharges the upper capacitor and the other half charges the lower capacitor, neither the upper diode nor the lower diode turns on. If no commutation capacitor were connected across each diode, a step change in the ac voltage of the diode rectifier would occur, due to the absence of the commutation interval of time depicted in Figs. 5(b) and 6(b). The instant that v_{CP} becomes equal to zero and v_{CN} to V_d, the ac current i_L begins to flow through the upper diode, as shown in Figs. 5(c) and 6(c).

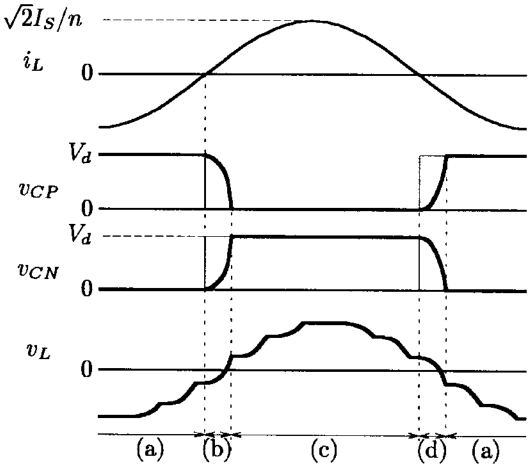

Fig. 6. Voltage and current waveforms, where the commutation capacitors are connected.

Comparison of the synthesized ac voltage v_L between Figs. 4 and 6 leads to the following conclusion. Connecting a commutation capacitor C across each diode is effective in reducing the peak voltage rating of the active filter, because a gradual change in v_L occurs during the overlapping of "voltage." The synthesized ac voltage has a dual relationship to the synthesized ac current in a conventional three-phase twelve-pulse diode rectifier with a small ac inductor and a large dc link inductor, which causes the overlapping of "current" during every interval time of commutation.

V. PEAK VOLTAGE RATING OF SERIES ACTIVE FILTER

Assuming that the primary-to-secondary voltage ratio of a transformer is $1 : n$ in a three-phase diode rectifier with a dc-link capacitor, and that the rms value of a sinusoidal ac current in the primary is I_S, the ac current in the secondary i_L is given by

$$i_L = \sqrt{2}\,\frac{I_S}{n}\sin \omega t. \tag{7}$$

During the commutation depicted in Fig. 6(b), the following equation exists between i_L and the voltage across the lower commutation capacitor v_{CN}:

$$v_{CN}(t) = \frac{1}{2C}\int_0^t i_L\,dt = \frac{I_S}{\sqrt{2}n\omega C}(1 - \cos \omega t). \tag{8}$$

The commutation ends when $v_{CN} = V_d$. This leads to determination of the commutation interval τ as follows:

$$\tau = \frac{1}{\omega}\cos^{-1}\left(1 - \frac{\sqrt{2}n\omega C}{I_S}V_d\right). \tag{9}$$

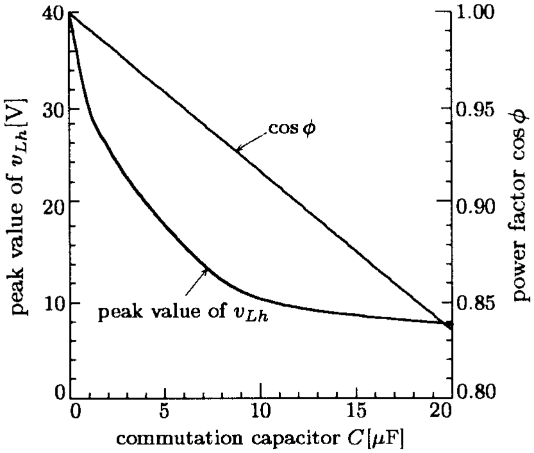

Fig. 7. Peak value of v_{Lh} and supply power factor $\cos\phi$ relative to capacitance values of the commutation capacitor.

Equations (8) and (9) enable us to obtain the ac terminal voltage relative to the dc-bus ground. For instance, the u-phase ac terminal voltage in the secondary of the Δ–Δ transformer, v_{CNu2} is given as follows:

$$v_{CNu2} = \begin{cases} \dfrac{I_S(1-\cos\omega t)}{\sqrt{2}n\omega C} & (0 \le t < \tau) \\ V_d & \left(\tau \le t < \dfrac{\pi}{\omega}\right) \\ V_d - \dfrac{I_S(1+\cos\omega t)}{\sqrt{2}n\omega C} & \left(\dfrac{\pi}{\omega} \le t < \dfrac{\pi}{\omega}+\tau\right) \\ 0 & \left(\dfrac{\pi}{\omega}+\tau \le t < \dfrac{2\pi}{\omega}\right) \end{cases}. \tag{10}$$

Based on (10), one obtains the three-phase ac terminal voltages in the secondary of the Y–Δ transformer, v_{CNu1}, v_{CNv1}, and v_{CNw1}, and those of the Δ–Δ transformer, v_{CNu2}, v_{CNv2}, and v_{CNw2}. Taking into account both the series connection of the primary windings and the primary-to-secondary voltage ratio of 1 : 2 in Fig. 1, the three-phase synthesized ac voltages of the double-series diode rectifier, v_{Lu}, v_{Lv}, and v_{Lw} are represented as follows:

$$\begin{bmatrix} v_{Lu} \\ v_{Lv} \\ v_{Lw} \end{bmatrix} = \frac{1}{2\sqrt{3}} \begin{bmatrix} 1 & 0 & -1 \\ -1 & 1 & 0 \\ 0 & -1 & 1 \end{bmatrix} \begin{bmatrix} v_{CNu1} \\ v_{CNv1} \\ v_{CNw1} \end{bmatrix} + \frac{1}{2} \begin{bmatrix} \frac{2}{3} & -\frac{1}{3} & -\frac{1}{3} \\ -\frac{1}{3} & \frac{2}{3} & -\frac{1}{3} \\ -\frac{1}{3} & -\frac{1}{3} & \frac{2}{3} \end{bmatrix} \begin{bmatrix} v_{CNu2} \\ v_{CNv2} \\ v_{CNw2} \end{bmatrix}. \tag{11}$$

Subtracting the fundamental voltage from v_L gives us the harmonic voltage produced by the double-series diode rectifier v_{Lh}.

It is easy to calculate the peak value of v_{Lh} by means of theoretical or numerical analysis of (9)–(11). Fig. 7 shows the peak value of v_{Lh} and the supply power factor $\cos\phi$ relative to the capacitance values of the commutation capacitor, where the line frequency is 60 Hz, the line-to-line voltage 200 V, and the rating of the double-series diode rectifier is 5 kW ($I_S = 15$ A, $V_d = 240$ V).

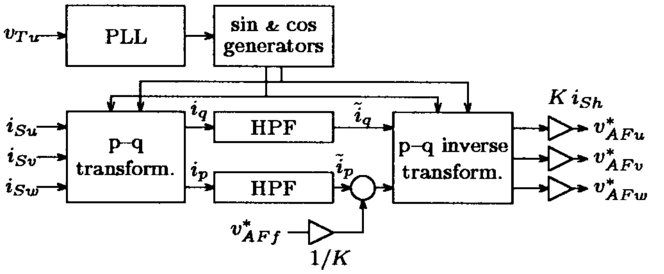

Fig. 8. Control circuit for the series active filter.

As the capacitance value of the commutation capacitor C is increased, the peak value of v_L decreases. Connecting the 5-μF commutation capacitor reduces the peak value by about 50%, compared to that without connecting any commutation capacitor. Fig. 7 implies, however, that connection of greater than 8-μF commutation capacitors is not effective in reducing the peak value, providing a constant peak value of about 10 V. The reason is that the commutation interval τ exceeds 30°, so that the overlapping of voltage occurs between both diode rectifiers. On the other hand, the supply power factor $\cos\phi$ linearly decreases from 1.00 to 0.84 in the range of $0 < C < 20$ μF. Fig. 7 concludes that an optimal capacitance value of the commutation capacitor exists between 5–8 μF.

Any capacitance value on the horizontal axis in Fig. 7 is applicable to another ac/dc power conversion system with different voltage, current, and frequency, attention being paid to (9). If another system has the same value in $\omega\tau$ as that of Fig. 1, it has the same voltage and current waveforms as Fig. 6. This leads to the following relation:

$$C \propto \frac{I_S}{n\omega V_d}. \tag{12}$$

Any peak value of v_{Lh} on the vertical axis in Fig. 7 is also applicable by multiplying the ratio of the supply line-to-line voltage of another system with respect to 200 V.

VI. CONTROL CIRCUIT

Fig. 8 shows a block diagram of a control circuit based on hybrid analog/digital hardware. The concept of the instantaneous active and reactive power theory or the so-called "p–q theory" [11] is applied to the control circuit implementation. The p–q transformation circuit executes the following calculation to convert the three-phase supply current i_{Su}, i_{Sv}, and i_{Sw} into the instantaneous active current i_p and the instantaneous active current i_q:

$$\begin{bmatrix} i_p \\ i_q \end{bmatrix} = \sqrt{\frac{2}{3}} \begin{bmatrix} \cos\omega t & \sin\omega t \\ -\sin\omega t & \cos\omega t \end{bmatrix} \begin{bmatrix} 1 & -\dfrac{1}{2} & -\dfrac{1}{2} \\ 0 & \dfrac{\sqrt{3}}{2} & -\dfrac{\sqrt{3}}{2} \end{bmatrix} \cdot \begin{bmatrix} i_{Su} \\ i_{Sv} \\ i_{Sw} \end{bmatrix}. \tag{13}$$

The fundamental components in i_{Su}, i_{Sv}, and i_{Sw} correspond to dc components in i_p and i_q and harmonic components to ac components. Two first-order high-pass filters (HPF's) with cutoff frequency of 10 Hz extract the ac components $\tilde{i}_p$ and $\tilde{i}_q$ from i_p and i_q, respectively [7]. Then, the p–q transformation/inverse transformation of the extracted ac components produces the following supply harmonic currents:

$$\begin{bmatrix} i_{Shu} \\ i_{Shv} \\ i_{Shw} \end{bmatrix} = \sqrt{\frac{2}{3}} \begin{bmatrix} 1 & 0 \\ -\frac{1}{2} & \frac{\sqrt{3}}{2} \\ -\frac{1}{2} & -\frac{\sqrt{3}}{2} \end{bmatrix} \cdot \begin{bmatrix} \cos\omega t & -\sin\omega t \\ \sin\omega t & \cos\omega t \end{bmatrix} \begin{bmatrix} \tilde{i}_p \\ \tilde{i}_q \end{bmatrix}. \qquad (14)$$

Each harmonic current is amplified by a gain of K, and then it is applied to the gate control circuit of the active filter as a voltage reference v^*_{AF}. In order to regulate the common dc-bus voltage, $v^*_{\mathrm{AF}f}$ is divided by the gain of K, and then it is added to $\tilde{i}_p$.

The phase-locked loop (PLL) circuit produces phase information ωt, which is a 12-bit digital signal of 60×2^{12} samples per second. Digital signals, $\sin\omega t$ and $\cos\omega t$, are generated from the phase information, and then they are applied to the p–q (inverse) transformation circuits. Multifunction in the transformation circuits is achieved by means of eight multiplying D/A converters. Each voltage reference v^*_{AF} is compared with two repetitive triangular waveforms of 10 kHz in order to generate the gate signals for the IGBT's. The two triangular waveforms have the same frequency, but one has polarity opposite to the other, so that the equivalent switching frequency of each inverter is 20 kHz, which is twice as high as that of the triangular waveforms.

VII. Experimental Results

In the following experiment, the control gain of the active filter K is set to 27 Ω, which is equal to 3.3 p.u. on a 3ϕ 200-V 15-A 60-Hz basis. Equation (2) suggests that the higher the control gain, the better the performance of the active filter. An extremely high gain, however, may make the control system unstable and, thereby, a tradeoff between performance and stability exists in determining an optimal control gain. A constant load resistor is connected to the common dc bus, as shown in Fig. 1.

A. In the Case of Connecting No Commutation Capacitor

Figs. 9 and 10 show experimental waveforms before and after the series active filter is started, respectively, where no commutation capacitor is connected. Table I shows the total harmonic distortion (THD) of i_S and the ratio of each harmonic current with respect to the fundamental current contained in i_S.

The waveforms of i_S and i_{L2} in Fig. 9 look like 12-ripple sinusoidal waveforms because commutation occurs every 30° in the double-series diode rectifier. Before starting the active filter, the third harmonic current of 5.4% flows into the diode rectifier because the third harmonic voltage of 1.5% is contained in the supply voltage v_S. The waveform of i_S in Fig. 9 does not meet the IEEE 519-1992 harmonic standards because the THD is 12.0%.

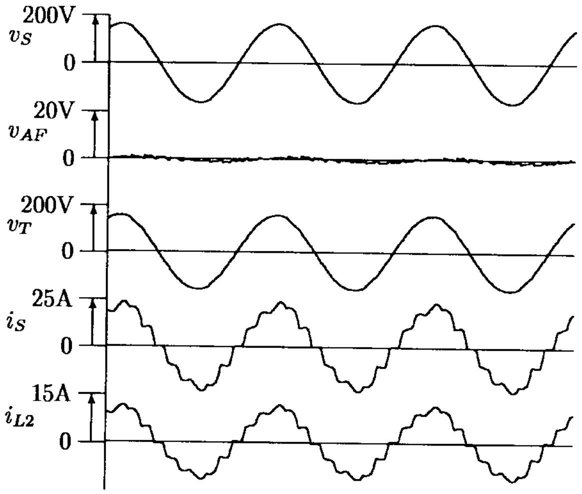

Fig. 9. Experimental waveforms before starting the series active filter, where no commutation capacitor is connected.

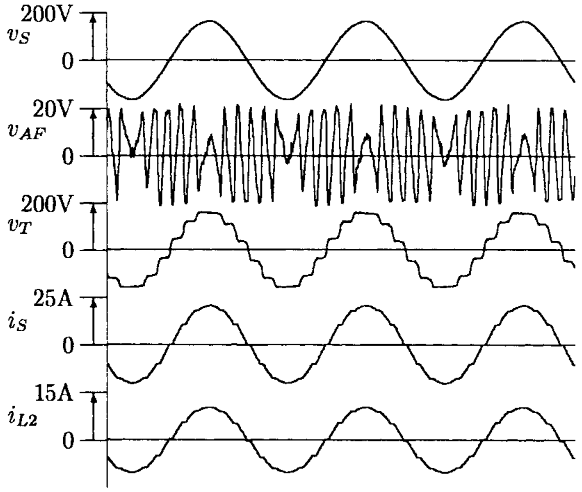

Fig. 10. Experimental waveforms after starting the series active filter with the output peak voltage limited within ±20 V, where no commutation capacitor is connected.

TABLE I
Supply Current THD and Harmonics Expressed as the Harmonic-to-Fundamental Current Ratio[%], Where no Commutation Capacitor is Connected

	THD	3rd	5th	7th	11th	13th
before (Fig. 9)	12.0	5.4	3.8	2.0	8.5	4.8
after (Fig. 10)	3.2	0.3	0.2	0.2	2.5	2.0

After starting the active filter, the waveform of i_S in Fig. 10 becomes almost sinusoidal, so that it perfectly meets the IEEE 519-1992 harmonic standards. Note that there is a distinct difference in v_T between Figs. 9 and 10. That is, Fig. 9 has a sinusoidal waveform because L_S is much smaller that L_L in Fig. 1. On the other hand, Fig. 10 has a 12-step waveform because the active filter supports the difference between the supply voltage v_S and the synthesized 12-step voltage depicted in Fig. 4, v_L, so that v_T becomes approximately equal to v_L. Because the peak output voltage of the active filter is 20 V in

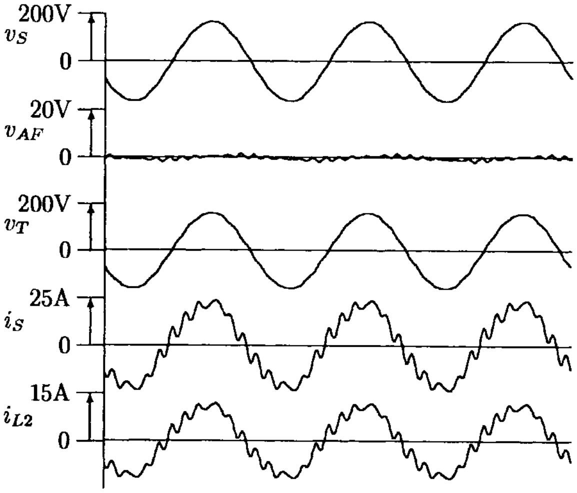

Fig. 11. Experimental waveforms before starting the series active filter, where commutation capacitors of 5 μF are connected.

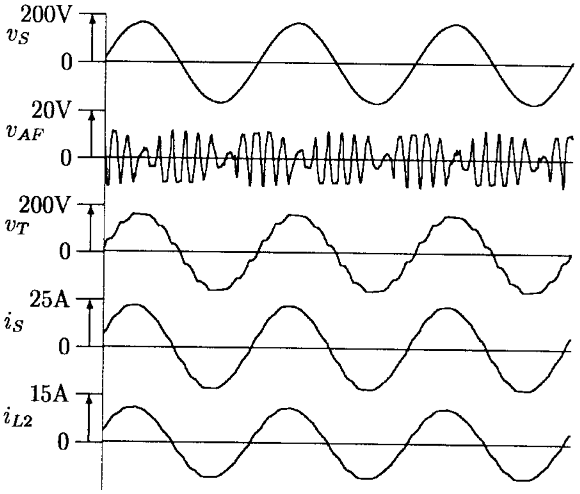

Fig. 13. Experimental waveforms after starting the series active filter with the output peak voltage limited within ±12 V, where commutation capacitors of 5 μF are connected.

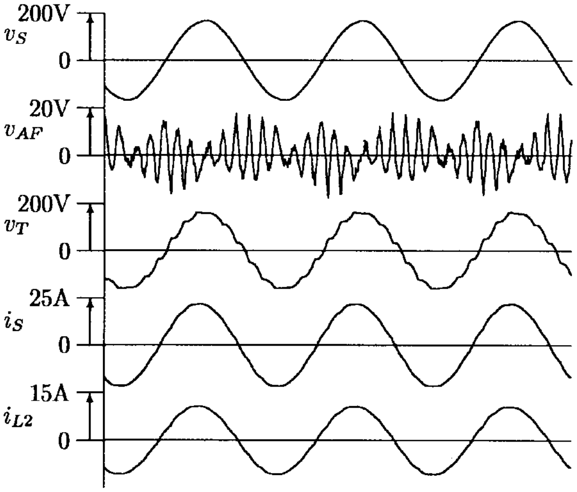

Fig. 12. Experimental waveforms after starting the series active filter with the output peak voltage limited within ±20 V, where commutation capacitors of 5 μF are connected.

TABLE II

Supply Current THD and Harmonics Expressed as the Harmonic-to-Fundamental Current Ratio[%], Where Commutation Capacitors of 5 μF are Connected

	THD	3rd	5th	7th	11th	13th
before (Fig. 11)	16.8	5.4	2.5	2.2	12.3	9.5
after (Fig. 12)	1.6	0.5	0.1	0.5	1.3	0.6
after (Fig. 13)	1.6	0.7	0.2	0.4	0.8	1.0

Fig. 10, the peak voltage and current rating is defined by

$$3 \times \left(\frac{20^{\rm V}}{\sqrt{2}}\right) \times 15^{\rm A} = 0.63\ {\rm kVA}. \tag{15}$$

B. In the Case of Connecting the Commutation Capacitors

Figs. 11–13 show experimental waveforms, where a 5-μF commutation capacitor is connected in parallel with each diode used for the double-series diode rectifier. Table II shows the THD of i_S and the ratio of each harmonic current with respect to the fundamental current contained in i_S.

Before starting the active filter, the supply eleventh and thirteenth harmonic currents in Fig. 11 are larger than those in Fig. 9, due to the resonance between the commutation capacitors C and the ac line and leakage inductors L_S and L_L [12]. As a result, the THD of i_S in Fig. 11 is 16.8%, while that in Fig. 9 is 12.0%. Nonnegligible amounts of third, fifth, and seventh harmonic currents, which are so-called "noncharacteristic current harmonics" for the three-phase twelve-pulse diode rectifier, are drawn from the utility.

After starting the active filter, a sinusoidal current with a leading power factor of 0.96 is drawn, because the active filter acts as a high resistor of 27 Ω, having the capability of compensating for both voltage harmonics V_{Sh} and V_{Lh}, as well as of damping the resonance. It is interesting to compare the waveform v_T between Figs. 10 and 12. A quick change in v_T occurs at every instant of commutation in Fig. 10, while a slow change occurs in Fig. 12. Thus, the peak voltage of $v_{\rm AF}$ reaches a saturation voltage of 20 V in Fig. 10 at every commutation, while it is 18 V in Fig. 12, without reaching the saturation voltage.

Fig. 13 shows experimental waveforms under the same conditions as those in Fig. 12, except that the peak voltage of the series active filter is imposed on a limitation of ±12 V inside the control circuit based on hybrid analog/digital hardware. Note that the limitation of ±12 V to the peak voltage is equivalent to the use of three single-phase matching transformers with turn ratio of 1 : 20 under the common dc-link voltage of 240 V. As shown in Fig. 13, the waveforms of i_S and v_T are not affected by the voltage limitation, although the peak voltage v_{AF} frequently reaches the saturation or limitation voltage of ±12 V. The reason is clarified in the following discussion. Comparing v_{AF} between Figs. 12 and 13 concludes that voltage saturation occurs only at the impulse part of v_{AF} during a short interval of time. This implies that the voltage saturation produces almost no effect on low-order, below the thirteenth, harmonic currents in i_S. In addition, the

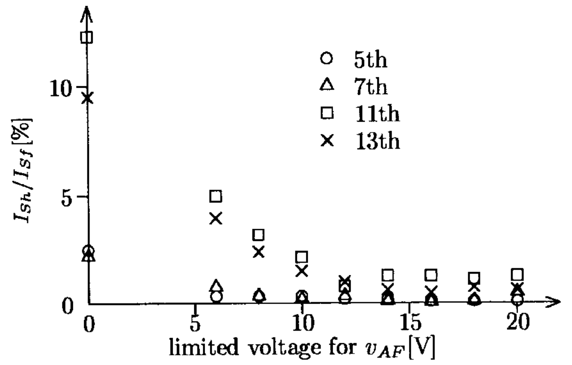

Fig. 14. Experimental results of relationships between voltage limitation of v_{AF} and supply current harmonics.

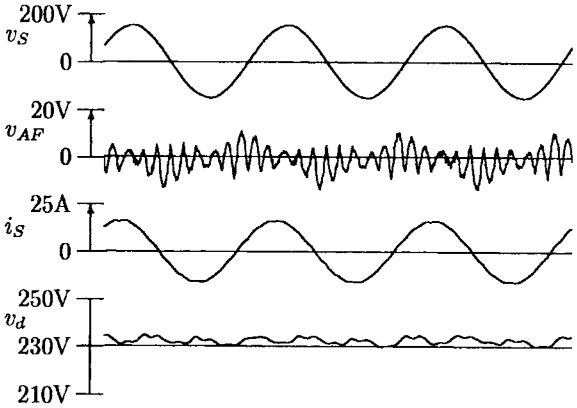

Fig. 15. Experimental waveforms with the common dc-bus voltage uncontrolled.

overlapping of voltage which occurs in each diode rectifier makes high-order, over the twenty-third, harmonic voltages in v_L extremely small. As a result, high-order, over the twenty-third, harmonic currents are negligible, due to the presence of the ac line and leakage inductors L_S and L_L. The required peak voltage and current rating of the series active filter in Fig. 13 is given by

$$3 \times \left(\frac{12^{\mathrm{V}}}{\sqrt{2}}\right) \times 15^{\mathrm{A}} = 0.38\,\mathrm{kVA}. \qquad (16)$$

Fig. 14 shows experimental relationships between voltage limitation and supply current harmonics, where voltage limitation in the range of ±6 to ±20 V is imposed on v_{AF} under a constant gain of $K = 27\,\Omega$. This verifies that voltage limitation in the range of ±12 to ±20 V produces almost no effect on fifth, seventh, eleventh, and thirteenth harmonic currents in i_S.

VIII. REGULATION OF COMMON DC-BUS VOLTAGE

Superimposing an amount of fundamental voltage on the compensating voltage given by (1) enables us to regulate the common dc-bus voltage. Fig. 15 shows experimental waveforms with the common dc-bus voltage of 233 V, when no fundamental voltage is superimposed.

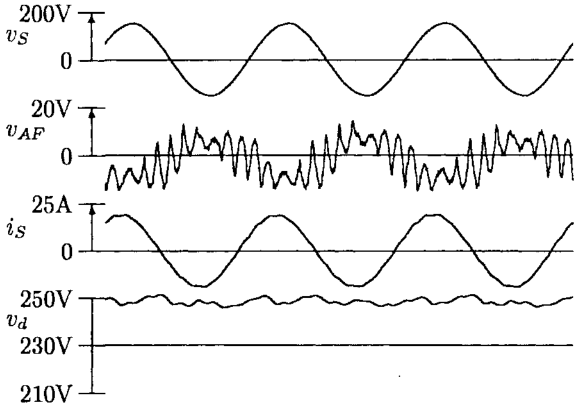

Fig. 16. Experimental waveforms with the common dc-bus voltage uncontrolled by 5%.

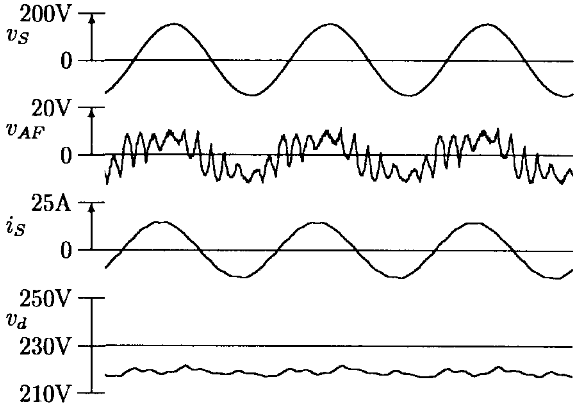

Fig. 17. Experimental waveforms with the common dc-bus voltage decreased by 5%.

Fig. 16 shows experimental waveforms when a 5% fundamental voltage is superimposed in phase with v_S for the purpose of increasing the common dc-bus voltage by 5%. Note that the positive direction of v_{AF} is opposite to that of the supply voltage v_S, as shown in Figs. 1 and 2. The supply current and the fundamental voltage applied by the active filter yield an amount of ac active power delivered from the common dc bus to the ac terminals of the active filter. The ac active power is converted to the dc power delivered to the common dc bus, thus circulating between the diode rectifier and the active filter. The electric power utility supplies all amount of active power delivered to the load connected on the common dc bus. In fact, the amplitude of i_S in Fig. 16 is a little bit larger than that in Fig. 15.

Fig. 17 shows experimental waveforms when the 5% fundamental voltage is superimposed in the opposite phase to v_S in order to decrease the common dc-bus voltage by 5%. Note that the supplementary value-added function of regulating the common dc-bus voltage within ±5% does not cause any increase in the peak voltage rating of the active filter, although it causes a slight increase in the rms voltage rating.

The compensating voltage injected by the active filter contributes to improving the power factor, due to a significant reduction of the supply current harmonics, but it produces no effect on the displacement factor, even in the case of voltage regulation.

IX. CONCLUSIONS

This paper has proposed a harmonic current-free ac/dc power conversion system which is capable of operating at a leading power factor of 0.96. The power circuit configuration is characterized by the integration of a small-rated series active filter with a large-rated double-series diode rectifier. The diode rectifier provides ac/dc power conversion, while the active filter achieves not only harmonic compensation, but also dc voltage regulation. The active filter integrated with the diode rectifier has the following functions:

- harmonic compensation of the diode rectifier;
- voltage regulation of the common dc bus;
- damping of harmonic resonance between the ac line and leakage inductors and the commutation capacitors;
- reduction of current ripples flowing into the electrolytic capacitor on the common dc bus.

Experimental results obtained from a 5-kW laboratory system have verified both the practical viability of the proposed system and the justification of the series active filter integrated with the diode rectifier. The harmonic current-free ac/dc power conversion system is expected to be used as a utility interface with large industrial inverter-based loads, such as multiple adjustable-speed drives and uninterruptible power supplies in the range of 1–10 MW.

REFERENCES

[1] T. Okuyama, H. Nagase, and Y. Kubota, “High performance ac motor speed control system using GTO converters,” in *Proc. 1983 Int. Power Electronics Conf.,* Tokyo, Japan, 1983, pp. 720–731.

[2] J. W. Dixon, A. B. Kulkarni, M. Nishimoto, and B. T. Ooi, “Characteristics of a controlled-current PWM rectifier-inverter link,” in *Proc. 1986 IEEE/IAS Annu. Meeting,* pp. 685–691.

[3] R. Wu, S. B. Dewan, and G. R. Slemon, “A PWM ac to dc converter with fixed switching frequency,” in *Proc. 1988 IEEE/IAS Annu. Meeting,* pp. 706–711.

[4] T. G. Habetler, “A space vector-based rectifier regulator for ac/dc/ac converters,” *IEEE Trans. Power Electron.,* vol. 8, pp. 30–36, Jan. 1993.

[5] F. Z. Peng, M. Kohata, and H. Akagi, “Compensation characteristics of shunt and series active filters,” in *Proc. 1992 Chinese–Japanese Power Electronics Conf.,* Beijing, China, 1992, pp. 381–387.

[6] H. Akagi, “New trends in active filters for power conditioning,” *IEEE Trans. Ind. Applicat.,* vol. 32, pp. 1312–1322, Nov./Dec. 1996.

[7] F. Z. Peng, H. Akagi, and A. Nabae, “A new approach to harmonic compensation in power systems—A combined system of shunt passive and series active filters,” *IEEE Trans. Ind. Applicat.,* vol. 26, pp. 983–990, Nov./Dec. 1990.

[8] L. Gyugyi and E. C. Strycula, “Active ac power filters,” in *Proc. 1976 IEEE/IAS Annu. Meeting,* pp. 529–535.

[9] L. Morán, P. Werlinger, J. Dixon, and R. Wallance, “A series active filter which compensates current harmonics and voltage unbalance simultaneously,” in *Proc. 1995 IEEE/PELS Power Electronics Specialist Conf.,* 1995, pp. 222–227.

[10] S. Bhattacharya and D. Divan, “Synchronous frame based controller implementation for a hybrid series active filter system,” in *Proc. 1995 IEEE/IAS Annu. Meeting,* 1995, pp. 2531–2540.

[11] H. Akagi, Y. Kanazawa, and A. Nabae, “Instantaneous reactive power compensators comprising switching devices without energy storage components,” *IEEE Trans. Ind. Applicat.,* vol. 20, pp. 625–630, May/June 1984.

[12] J. G. Kassakian, M. F. Schlecht, and G. C. Verghese, *Principles of Power Electronics.* Reading, MA: Addison-Wesley, 1991, p. 77.

Hideaki Fujita (M’91) was born in Toyama Prefecture, Japan, in 1965. He received the B.S. and M.S. degrees in electrical engineering from Nagaoka University of Technology, Nagaoka, Japan, in 1988 and 1990, respectively.

Since 1991, he has been a Research Associate in the Department of Electrical Engineering, Okayama University, Okayama-City, Japan. His research interests include static var compensators, active power filters, and resonant converters.

Mr. Fujita received First Prize Paper Awards from the Industrial Power Converter Committee of the IEEE Industry Applications Society in 1990 and 1995.

Hirofumi Akagi (M’87–SM’94–F’96) was born in Okayama-City, Japan, in 1951. He received the B.S. degree from Nagoya Institute of Technology, Nagoya, Japan, in 1974 and the M.S. and Ph.D. degrees from the Tokyo Institute of Technology, Tokyo, Japan, in 1976 and 1979, respectively, all in electrical engineering.

In 1979, he joined Nagaoka University of Technology, Nagaoka, Japan, as an Assistant Professor in the Department of Electrical Engineering. He later became an Associate Professor. Since 1991, he has been a Full Professor in the Department of Electrical Engineering, Okayama University. He was a Visiting Scientist at Massachusetts Institute of Technology (MIT), Cambridge, for ten months in 1987. From March to August 1996, he was a Visiting Professor at the University of Wisconsin, Madison, and MIT. His research interests include ac motor drives, high-frequency resonant inverters for induction heating and corona discharge treatment, and utility applications of power electronics, such as active filters, static var compensators, and FACTS devices.

Dr. Akagi has received six IEEE Industry Applications Society and Committee Prize Paper Awards, including the First Prize Paper Award in the IEEE TRANSACTIONS ON INDUSTRY APPLICATIONS for 1991.